Heat transfer in a simulated spent fuel pool for different types of spent fuels

Transferência de calor em um pool simulado de combustível queimado para diferentes tipos de combustíveis queimados

DOI:10.34117/bjdv9n1-343

Recebimento dos originais: 23/12/2022
Aceitação para publicação: 25/01/2023

Fernando Pereira de Faria
Doctor of Physics
Institution: Universidade Federal de Minas Gerais
Address: Av. Antônio Carlos, 6627, Pampulha, Belo Horizonte - MG, Brasil, CEP: 31270-901
E-mail: fernandopereirabh@gmail.com

Dario Martin Godino
Doctor of Engineering
Institution: Centro de Investigación de Métodos Computacionales (CIMEC), UNL, CONICET, FICH, Santa Fe, Argentina
Address: Ruta Nac Nro 168, Km 0, Paraje El Pozo, 3000, Santa Fe - Argentina
E-mail: dmgodino@gmail.com

Santiago Francisco Corzo
Doctor of Engineering
Institution: Centro de Investigación de Métodos Computacionales (CIMEC), UNL, CONICET, FICH, Santa Fe, Argentina
Address: Ruta Nac Nro 168, Km 0, Paraje El Pozo, 3000, Santa Fe, Argentina
E-mail: santiagofcorzo@gmail.com

Damián Enrique Ramajo
Doctor of Engineering
Institution: Centro de Investigación de Métodos Computacionales (CIMEC), UNL, CONICET, FICH, Santa Fe, Argentina
Address: Ruta Nac Nro 168, Km 0, Paraje El Pozo, 3000, Santa Fe, Argentina
E-mail: dramajo@santafe-conicet.gov.ar

Antonella Lombardi Costa
Doctor in Nuclear and Industrial Security
Institution: Universidade Federal de Minas Gerais
Address: Av. Antônio Carlos, 6627, Pampulha, Belo Horizonte - MG, Brasil, CEP: 31270-901
E-mail: antonella@nuclear.ufmg.br

Cláubia Pereira Bezerra Lima
Doctor in Environment and Nuclear Safety
Institution: Universidade Federal de Minas Gerais
Address: Av. Antônio Carlos, 6627, Pampulha, Belo Horizonte - MG, Brasil,
CEP: 31270-901
E-mail: claubia@nuclear.ufmg.br

ABSTRACT
Historically, the Spent Fuel Pool (SFP) of Angra II, from Brazil, has received standard spent fuel (SF) assemblies of uranium dioxide (UO_2) discharged from Pressurized Water Reactors (PWR) of the Nuclear Power Plants (NPP) of Angra. However, in case of using Mixed Oxide (MOX) or thorium-based fuels at a proportion of 1/3 or 1/4 of the total of fuel assemblies in their PWRs as it has been occurring worldwide, it would require further thermal studies of wet storage of the new mixed SF generated. It includes the determination of the water boiling time (T_b) of the SFP in case of breakdown of its external cooling system (ECS). This work presents studies of T_b of a simulated SFP storing mixed SF discharged from PWRs. The types of mixed SF studied include MOX plus UO_2, oxide of thorium/uranium $(U\text{-}Th)O_2$ plus UO_2, and oxide of thorium/transuranic $(TRU\text{-}Th)O_2$ plus UO_2. All the mixed SF was considered to contain 1/3 or 1/4 of either thorium-based fuels or reprocessed fuel. The simulations were implemented in CFX Ansys and OpenFOAM© codes. T_b from simulations with Ansys ranged from 4.05 h to 5.97 h, and from 3.45 h to 5.77 h from simulations with OpenFOAM©. Results show that, independent of the mixed loading pattern of the SFP, the water would reach the saturation temperature more rapidly when $(TRU\text{-}Th)O_2$ was present. By contrast, when MOX was present, T_b was greater.

Keywords: Spent fuel pool, OpenFOAM©, CFX Ansys.

RESUMO
Historicamente, o Pool de Combustível Irradiado (SFP) de Angra II, do Brasil, tem recebido montagens de combustível padrão gasto (SF) de dióxido de urânio (UO2) descarregado de Reatores de Água Pressurizada (PWR) das Usinas Nucleares (NPP) de Angra. Entretanto, no caso de utilização de combustíveis à base de óxido misto (MOX) ou tório na proporção de 1/3 ou 1/4 do total de conjuntos de combustível em suas PWRs como vem ocorrendo em todo o mundo, seriam necessários mais estudos térmicos de armazenamento úmido do novo SF misto gerado. Inclui a determinação do tempo de ebulição da água (Tb) do SFP em caso de quebra de seu sistema de resfriamento externo (ECS). Este trabalho apresenta estudos de Tb de um SFP simulado de armazenamento de SF misto descarregado de PWRs. Os tipos de SF mistos estudados incluem MOX mais UO2, óxido de tório/urânio (U-Th)O2 mais UO2, e óxido de tório/transurânico (TRU-Th)O2 mais UO2. Todo o SF misto foi considerado como contendo 1/3 ou 1/4 de combustíveis à base de tório ou combustível reprocessado. As simulações foram implementadas nos códigos CFX Ansys e OpenFOAM©. Tb de simulações com Ansys variou de 4,05 h a 5,97 h, e de 3,45 h a 5,77 h de simulações com OpenFOAM©. Os resultados mostram que, independente do padrão de carga mista do SFP, a água alcançaria a temperatura de saturação mais rapidamente quando (TRU-Th)O2 estivesse presente. Em contraste, quando MOX estava presente, a Tb era maior.

Palavras-chave: Pool de combustível gasto, OpenFOAM©, CFX Ansys.

1 INTRODUCTION

Aiming at decreasing the utilization of uranium, some nuclear utilities are planning, or have already implemented plutonium recycling schemes in thermal reactors, specially, PWRs. Normally, plutonium is recycled as MOX fuel, in which it is mixed with UO_2 in the form of plutonium dioxide (PuO_2) in a same reactor at a proportion of 1/3 or 1/4 [1]. Since 80's, France has been reprocessing SF and recycling the fuel obtained from Pu spiked with depleted uranium (MOX), and inserting it into its reactors. Such a policy was also adopted by other European countries and by Japan [2]. Another kinds of mixed fuels have been investigating e.g., oxides of thorium/uranium, thorium/plutonium, thorium/transuranic, and transuranic/uranium [1,3-6]. Recently, researchers have been turning their attention to Th fuel cycle in PWRs aiming at reducing the generation of minor actinides, at improving the nuclear power sustainability, and at better fuel utilization and breeding [7-9]. Studies have also discussed the possible role of Th utilization in power reactors and the associated fuel cycles [10].

After reactor discharge, SF must remain under wet storage into SFP until the temperature and the radioactivity emission drop off to safety values for transportation to the final repository. The SFP temperature is controlled by an ECS beneath pre-determined values established according to each country regulation [11], which, typically, should remain between 298 K and 310 K. The Brazil's SFP was designed to store UO_2-SF discharged from PWRs of the nuclear power plants of ANGRA I and II. The knowledge of the temperature temporal behaviour in an hypothetical scenario of breakdown of the ECS is a requirement for SFP's licensing. Such behaviour is already well-known for the standard UO_2. However, further analysis including criticality and thermal studies must be conducted for SF originated from thorium-based fuels and reprocessed fuels in view of their possible future utilization in national PWRs.

Concomitant to studies of criticality safety analysis, this research group have been employing efforts to develop thermal simulation studies considering a future scenario of mixed loading pattern of SF into the SFP.

The present work presents thermal studies in the absence of an ECS of the SFP. The modelled SFP follows the loading patterns of assemblies containing mixed SF, which is composed by either (U-Th)O_2 plus UO_2 or (TRU-Th)O_2 plus UO_2 or MOX plus UO_2. T_b from such scenarios are also compared with the standard loading of UO_2-SF. The studies were implemented in the Ansys CFX and OpenFOAM© codes.

1.1 THE SFP OF ANGRA II: PREVIOUS SIMULATIONS OF CRITICALITY SAFETY ANALYSIS

The main characteristics of the SFP are detailed in the Final Safety Analysis Report - FSAR [12]. Its dimensions are 15.914 m x 5.668 m, and 11.6568 m in depth. The fuels assemblies are arranged into the pool in storage racks, obeying the subcriticality regime.

This research group have performed simulations of criticality safety analysis for three different loading patterns designed for assemblies while into the pool [13]. Firstly, a loading pattern with only UO_2 SF was studied. Another analysis considered the SFP fully filled with assemblies of SF, being a quarter of MOX, (Th-U)O_2, (TRU-Th)O_2 or (TRU-U)O_2, and three quarters of standard UO_2-SF, i.e., a proportion 1:3. Lastly, a loading pattern with the proportion 1:2 was studied, being one assembly of MOX, (Th-U)O_2, (TRU-Th)O_2 or (TRU-U)O_2 together with two standard UO_2-SF assemblies. Figure 1 shows the smallest part of these patterns, called throughout the text as Unit of Repetition (UR), which are replicated until the SFP is fully filled.

The maximum numbers of assemblies into the pool were obtained using a 0.695 cm pitch distance, and maintaining the criticality under the upper multiplication factor limit of 0.95, according to the FSAR [12, 13].

The number of assemblies was 1252 when SFP was entirety filled with only UO_2-SF. The total of assemblies in the simulated cases were 313 of MOX, (Th-U)O_2, (TRU-Th)O_2 or (TRU-U)O_2, and 939 assemblies of UO_2-SF for the loading pattern with proportion 1:3. These numbers were 418 of MOX, (Th-U)O_2, (TRU-Th)O_2 or (TRU-U)O_2 and 834 assemblies of UO_2-SF in the pattern with proportion 1:2 [13].

Figure 1. Examples of a unit of repetition of two mixed loading patterns into the pool. The green points arranged in a square lattice represent MOX, (Th-U)O_2, (TRU-Th)O_2 or (TRU-U)O_2 assemblies of SF. Remaining assemblies are of UO_2-SF. Adapted from [13]

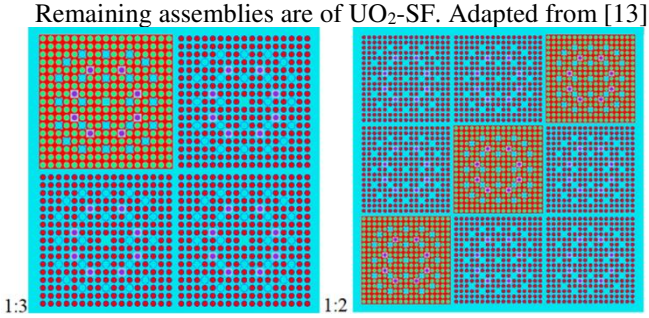

2 DESCRIPTION OF THE MODEL

This section details the SF properties that are heat sources into the pool. It also describes the geometry of the model, thermophysical properties, boundary and initial conditions, and the meshing of the geometry.

2.1 SPENT FUELS PROPERTIES

The main characteristics of SFs include the final amount of fissile material, the burnup and the operation time of reactor were obtained from [13], and are listed in following:

- UO_2: enriched to 4.3 w/o 235U/U; burnup of 48 GWd/tHM during 3.61 years and 1.634% of final amount of fissile material.
- (TRU-Th)O_2: fuel composed of 10% of Th and 90% of reprocessed fuel by UREX+, with 9.53% of fissile material; burnup of 48 GWd/tHM during 3.61 years and 6.657% of final amount of fissile material.
- MOX: enriched to 0.25 w/o 235U/U; burn-up of 48 GWd/tHM during 3.61 years and 3.375% of final amount of fissile material.
- (U-Th)O_2: Enriched to 4.869 w/o 235U/U; burn-up of 48 GWd/tHM during 3.61 years and of 2.084% final amount of fissile material.

2.2 GEOMETRY

In this work, the simulated SFP is a representation of the real Angra II pool from Brazil. Each assembly of SF is modelled as a solid cylinder, and only a single UR is represented. To determine the volume of water in the model, the proportion SF/water in the real pool fully filled with assemblies was adopted.

According to the previous studies of criticality safety analysis [13], the maximum volumes of SF into the pool in a loading pattern 1:2 are 20.74 m^3 of reprocessed fuel and 42 m^3 of UO_2, and the volume of water is approximately 1,235 m^3. Therefore, the proportion SF/water is around 0.0508, which is the same in the mixed loading 1:2. Figure 3 shows the modelled SFP that contains a single UR with loading patterns 1:2 and 1:3.

Figure 3. The modelled SFP containing blue cylinders that represent assemblies of (TRU-Th)O_2 or (U-Th)O_2 or MOX, and grey cylinders representing assemblies of UO_2

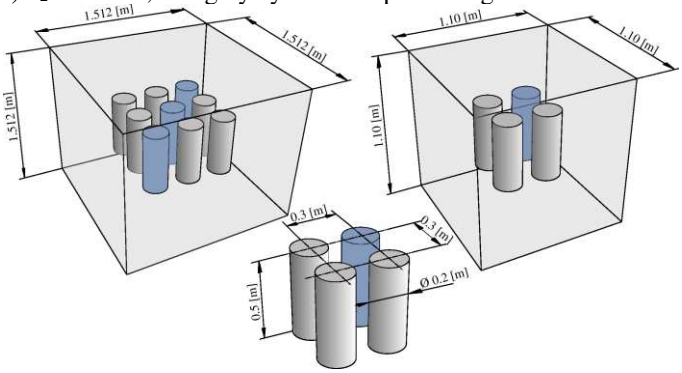

2.3 SIMULATED CASES

The following studies were addressed considering the modelled SFP loaded according to the pattern 1:2:

- Case I: three cylinders of (TRU-Th)O_2 and six of UO_2
- Case II: three cylinders of (U-Th)O_2 and six of UO_2
- Case III: three cylinders of MOX and six of UO_2
- Case IV: nine cylinders of UO_2

For the SFP filled according to the pattern 1:3:

- Case V: one cylinder of (TRU-Th)O_2 and three of UO_2
- Case VI: one cylinder of (U-Th)O_2 and three of UO_2
- Case VII: one cylinder of MOX and three of UO_2
- Case VIII: four cylinders of UO_2

2.4 HEAT SOURCES

The heat sources were derived from the decay heat profiles of the SF, at time t=0 year after reactor discharge [13]. To convert from [W/tHM] to [W/m3], the values were multiplied by the SF densities. Table 1 shows the heat sources values and their densities.

Table 1. The heat sources values

SF type	**Density (kg/m^3)**	***Heat source-1** x10^5 **(W/m^3)**	****Heat sources-2** x10^5 **(W/m^3)**
[a] UO_2	10830	3.24537	3.24537
[b] UO_2		2.08821	2.37162
(TRU-Th)O_2	11400	6.86987	6.07654
(U-Th)O_2	9510	3.67415	3.49903
MOX	10873	3.10441	3.15659

(*) and (**) are values for the patterns 1:2 and 1:3, respectively
(a) Only UO_2; (b) UO_2 together with SF from reprocessed fuels

2.5 MESHING DATA

The meshes were performed with Ansys CFX meshing tools, and with OpenFOAM© tools. The domains were meshed in different element sizes, depending on their dimensions. Figure 4 shows the mesh of the geometry for the arrangement of nine cylinders (pattern 1:3). The same mesh was used for the arrangement of four cylinders (pattern 1:2).

Figure 4. An illustration of the meshing. The figure is not to scale

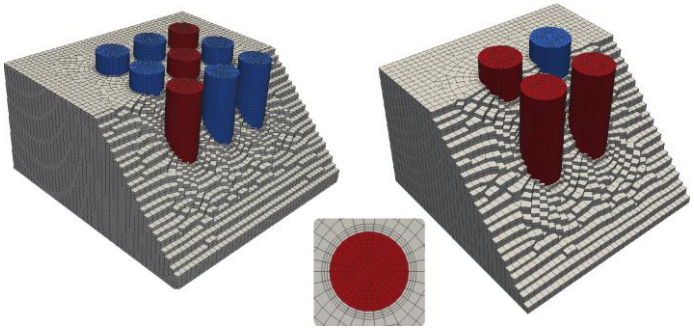

Studies of spatial grid convergence were carried out following the Roche's method that is based on the Richardson's extrapolation (ER) [14, 15], and it was applied to the case VIII. The mesh considered appropriated for this case was also used in all other cases. The method requires two or more successively finer grids with a constant grid refinement ratio, r. It was adopted r = 2, such that N1 = r N2 = r^2 N3, with N being the number of volumetric elements of the domain. Remembering that as greater is N as finer is the grid, and the grid spacing approaches to zero. Table 2 summarizes the data. The column named as "Normalized grid" corresponds to the mesh normalized by the number of elements of the finer grid to which was attributed the index "1".

Table 2. Data of spatial grid convergence

Normalized grid	**Nwater**	**Nfuels**	**T_b (h)**
1	86720	24960	4.845
2	43360	12480	4.857
4	21680	5852	4.902

Nwater: number of elements of the pool. Nfuels: total number of elements of the cylinders.

The ER may be used to estimate the value of a quantity of interest, *f*, at grid spacing *h* = 0. In our studies, *f* = T_b. For r = 2, ER may be written as:

$$f_{h=0} \cong \frac{4}{3}\left[f_1 - \frac{1}{4} f_2 \right] \quad (1)$$

The grid convergence index (GCI) was applied to verify the solution convergence. It is a measure of the percentage that computed values are away from the value of the asymptotic numerical value. It also indicates an error band on how far the solution is from the asymptotic value, and indicates how much the solution would change with a further refinement of the grid. A small value of GCI indicates that the computation is within the asymptotic range. GCI is computed considering values from sequential grids as follows,

$$GCI_{i,i+1} = 1.25 \frac{\left[\frac{f_i - f_{i+1}}{f_i} \right]}{r^p - 1} \quad (2)$$

where 1.25 is a factor of safety for comparisons over three or more grids, and p is the solution's order of convergence computed for three sequential grids with the expression:

$$p = \ln\left[\frac{f_3 - f_2}{f_2 - f_1} \right] \Big/ \ln(r) \quad (3)$$

The quantity asymptotic value is assumed to have been reached when,

$$\frac{GCI_{23}}{r^p GCI_{12}} \cong 1 \quad (4)$$

Table 3 summarizes the preliminary grid convergence analysis.

Table 3. Main values of the grid convergence analysis

Quantities	Value
GCI_{12}	(*)0.113
GCI_{23}	(*)0.421
p	1.91

(*) is in %. p is the order of convergence

From table 3, the eq. (4) is approximately 1.00248, i.e., the solutions from grids 1, 2 and 3 are within the asymptotic range of convergence. Figure 5 shows the behaviour of T_b versus the normalized grid (Table 2).

In light of these preliminary studies, the simulated cases V to VIII belonging to the loading pattern 1:3 were meshed according to the grid labelled as "grid 1" (Table 3). For cases I to IV, the parameters were maintained, including the element sizes. The number of elements was 5852 elements in each cylinder of SF, and 175641 elements for the pool. The pool element size was 3.7 x 10^{-2} m. Each cylinder was meshed by means of the number of division tool on its lids, totalling 42 divisions. The main quality parameters of the mesh are listed in Table 4.

Table 4. Main quality parameters of the adopted mesh

Domain	**Maximum aspect of ratio**	**Maximum no-ortogonality**	**Average no-ortogonality**	**Maximum skewness**
Cylinders of SF	5.41	20.76	3.54	0.532
Water	5.43	24.62	3.36	

2.6 THERMOPHYSICAL PROPERTIES OF MATERIALS

The water properties are from [16], at 298 K. The UO_2 properties, at 673 K, are from [17]. The molar mass of MOX, (U-Th)O_2, (TRU-Th)O_2 and (U-Th)O_2 were estimated from their chemical compositions from [13], at 298 K.

The remaining MOX properties are arithmetic means of values between 600 K and 700 K from [18]. The density, specific heat and thermal conductivity of (U-Th)O_2, at 673 K, are from [19], while its thermal expansivity is from [20] at this temperature.

Figure 5. T_b versus normalized grid. Plot shows the prediction of T_b at a continuous grid (h=0) according to the ER extrapolation (Eq. 1)

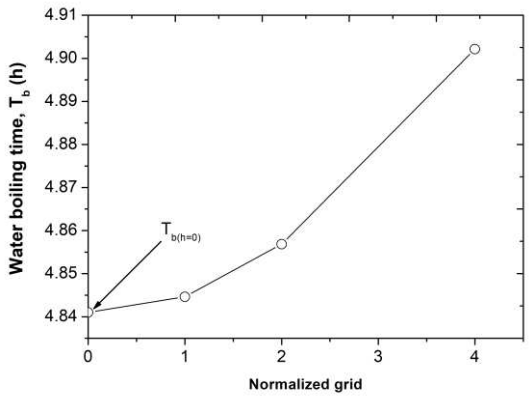

The (TRU-Th)O_2 properties were estimated considering the most significant dioxides present in its composition, which are ThO_2, PuO_2 and UO_2 [13]. The density, specific heat, conductivity, and thermal expansivity are represented by Q, and were estimated by the following expression:

$$Q_{(TRU-Th)O_2} = \frac{xQ_{(ThO_2)} + yQ_{(PuO_2)} + zQ_{(UO_2)}}{x+y+z} \quad (5)$$

where x, y and k are the fractions of ThO_2, PuO_2 and UO_2, respectively. These fractions were obtained from [13], whose values are 0.74, 0.093, 0.013, respectively. The dioxides properties were derived from [17, 19], and are arithmetic means in the temperature range from 600 K to 700 K. The properties values are summarized in table 5.

2.7 BOUNDARY AND INITIAL CONDITIONS

The k-epsilon turbulence and buoyancy models were adopted in the pool domain, whose walls, including the top, were set as adiabatic. The pressure in water was set as 1 atm. The initial temperatures were: 298 K for water and 673 K for cylinders of SF. The latter value is the temperature of an assembly of SF at the nuclear reactor shutdown.

T_b is the mean temperature of the water, being averaged over the whole water volume. Figure 6 shows the main boundary and initial conditions of the model.

Figure 6. The boundary and initial conditions of the model

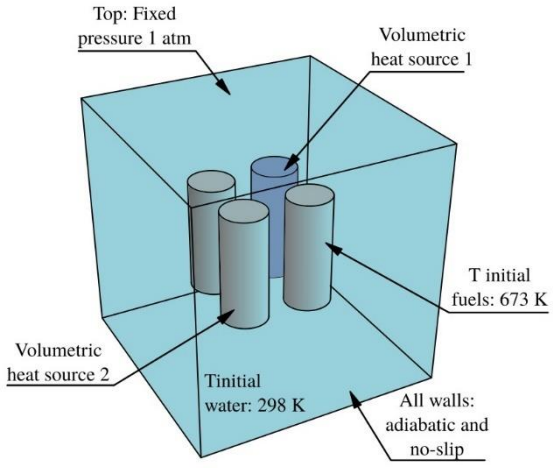

Table 5. Thermophysical properties of materials

SF type	Density [kg/m^3]	Molar mass [kg/kmol]	Specific heat [J/(kg.K)]
*Water	997.1	18.02	4183
UO_2	10830	270	297
(TRU-Th)O_2	11400	265	276.5
(U-Th)O_2	9510	202.83	362.4
MOX	10873	207	297.9

SF type	λ [W/(m.K)]	Thermal expansivity x10^{-6} [K^{-1}]
Water	0.5948	259.4
UO_2	4.74	10
(TRU-Th)O_2	3.065	8.604
(U-Th)O_2	5.2	8.0
MOX	2.48	9.9

3 RESULTS AND DISCUSSION

The results were compared among them by using both ANSYS CFX and OpenFOAM© codes.

3.1 T_B FROM SIMULATIONS WITH LOADING PATTERN 1:2: CASES I, II, III, AND IV

Cases I, II, III represent mixed storages, where the three cylinders of SF of a single diagonal (see Figure 1, right) are either (TRU-Th)O_2 or (U-Th)O_2, or MOX, and the remaining are UO_2. Case IV is the standard storage with only UO_2.

Figure 7 shows the temporal behaviour of the water temperature in the absence of an ECS for the pool. T_b from each case is listed on Table 6. ΔT_b is the difference between T_b obtained from each case and the standard case of UO_2 (case IV).

3.2 T_B FROM SIMULATIONS WITH LOADING PATTERN 1:3: CASES V, VI, VII, AND VIII

Cases from V, VI and VII represent mixed storages, where one of the four cylinders of SF is (TRU-Th)O_2 or (U-Th)O_2, or MOX, and the remaining are UO_2 (see Figure 1, left). Case VIII is the standard storage with only UO_2.

Figure 8 shows the temporal behaviour of the water temperature. T_b from each case is listed on Table 7.

As expected, T_b values from loading pattern 1:2 are lower than those ones when SFP is loaded following the pattern 1:3 since there is more heat being transferred to the water in the arrangement containing more assemblies of reprocessed fuels.

Even though the heat source value of the (U-Th)O_2 SF is higher compared to that of UO_2, (Table 1), T_b from the cases of (U-Th)O_2 together with UO_2 is greater than T_b from the cases with only UO_2 in both loading patterns. This observation can be explained by the higher specific heat value of the (U-Th)O_2 in comparison to that of UO_2 (Table 5). The same observation can be verified for the case VII (MOX together with UO_2). In light of the heat source value of MOX (Table 1), T_b would be lower than that from the case VIII (only UO_2). However, as can be seen in table 5, thermal conductivity, λ, of MOX is lower than that of UO_2. Although its specific heat is higher, in this situation, it seems that λ has the major influence in the heat propagation.

As can be seen from Figures 7 and 8, the smallest differences between ANSYS and OpenFOAM© results are verified for simulations with only UO_2. In simulations with two heat sources, the divergence between the codes enhanced with the time. The present studies are unable to explain such differences since all the simulation parameters are essentially the same in both codes. Further studies will be necessary to clarify it.

In both SFP's loading patterns, the difference (ΔT_b) between T_b from each simulated case and the standard case of UO_2 has the higher value for MOX (tables 6 and 7), whilst the mixed loading of (TRU-Th)O_2 together with UO_2 has the lowest ΔT_b. It means that, in case of breaking down of the ECS, SFP would reach the saturation temperature more quickly when it is loaded with the combination of (TRU-Th)O_2 and UO_2, and it would take more time to reach this temperature when loaded with the combination of MOX and UO_2, independent of the loading pattern.

Table 6. T_b from the loading pattern 1:2 – Cases from I to IV

Cases	**T_b (h)**		**ΔT_b (min)**	
	Ansys	Open FOAM	Ansys	Open FOAM©
I	4.05	3.48	-28.8	-51.6
II	5.27	4.67	44.4	19.8
III	5.89	5.21	81.6	52.2
IV	4.53	4.34	-----	-----

Figure 8. T_b versus normalized grid. Plot shows the prediction of T_b at a continuous grid (h=0) according to the ER extrapolation (Eq. 1)

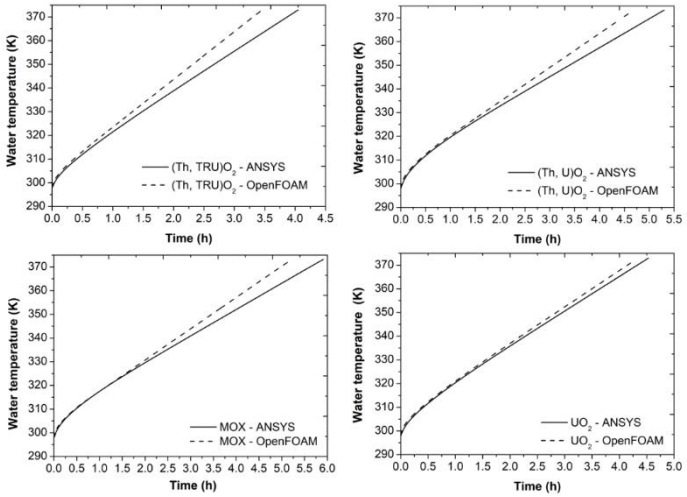

Table 7 T_b from the loading pattern 1:3– Cases from VI to VIII.

Cases	**T_b (h)**		**ΔT_b (min)**	
	Ansys	Open FOAM	Ansys	Open FOAM©
V	4.78	4.25	-1.8	21.6
VI	5.79	5.40	58.8	47.4
VII	5.97	5.77	69.6	69.6
VIII	4.81	4.61	-----	-----

Figure 7. Water temperature behaviour when SFP is loaded according to the pattern 1:3

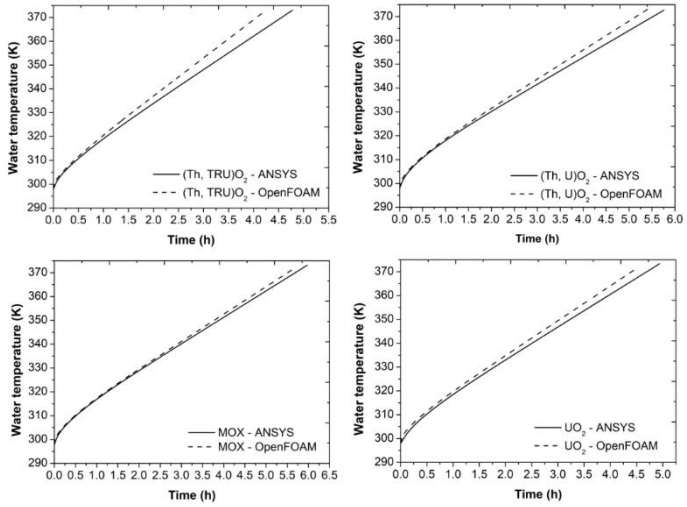

4 CONCLUSION

This work presented studies of the time in which a simulated spent fuel pool takes to reach the water boiling time in the absence of an external cooling system. Three different loading patterns of spent fuel assemblies were studied. The modelled pool is a

simplification of that from Angra II, Brazil, and consisted on a smallest unit of repetition of its loading patterns.

It was verified that when the simulated spent fuel pool was loaded with (TRU-Th)O_2 together with UO_2, it reaches 373 K more quickly than any other kind of loading. In contrast, it takes more time to reach this temperature when the loading is with MOX together with UO_2. The differences found in the water boiling times resulted from a balance between the heat source intensities, specific heat and thermal conductivity of the spent fuels.

The simulations were carried out with two codes – ANSYS and OpenFOAM©. Both yielded similar results, although major differences were observed in results from simulations with two different heat sources. Additional studies might be required to investigate these differences.

ACKNOWLEDGMENTS

The authors are greateful to the Coordenação de Aperfeiçoamento de Pessoal de Nível Superior (CAPES), to Fundação de Amparo à Pesquisa do Estado de Minas Gerais (FAPEMIG), and to Conselho Nacional de Desenvolvimento Científico e Tecnológico (CNPq) for the support.

REFERENCES

[1] Organization for Economic Co-operation and Development ECD/NEA. Physics of Plutonium Recycling. 2011. *Available from: https://www.oecd-nea.org/science/wprs/wppr/intro.html*

[2] Fukuda K., Choi J.S., Shani R., Durpel L.V.D., Berel E., Sartori E., MOX fuel use as a Back-End Option: Trends, Main Issues and Impacts on Fuel Cycle Management, *Vienna: IAEA-SM-358/I*, 2000, pp. 6-25

[3] Pereira C., Leite E.M., Non-Proliferating Reprocessed Nuclear Fuels In Pressurized Water Reactors: Fuel Cycle Options, *Annals of Nuclear Energy,* Vol. 25, 1998, pp. 937-62

[4] Pereira C., Leite E.M., Faria E.F., Waste analysis generated by alternative reprocessing fuels from pressurised water reactions, *Annals of Nuclear Energy*, Vol. 27, 2000, pp.449-64

[5] Monteiro F.B.A., De Faria R.B., Fortini M.A., Da Silva C.A., Pereira C., Assessment of the insertion of reprocessed fuels and combined thorium fuel cycles in a PWR system, *MRS Proceedings*, 2015, 1769: IMRC 2014 6E-13

[6] Monteiro F.B.A., Castro V.F., De Faria R.B., Fortini M.A., Da Silva C.A., Pereira C., Micro heteregeneous approaches for the insertion of reprocessed and combined thorium fuel cycles in a PWR system, *MRS Proceedings*, 2016, 1814: Imrc2015sim28-abs012

[7] Maiorino J.R., Stefani G.L., Moreira J.M.L., Rossi P.C.R., Santos T.A., Feasibility to convert an advanced PWR from UO_2 to a mixed U/ThO_2 core – Part I: Parametric studies, *Annals of Nuclear Energy*, Vol. 102, 2017, pp. 47-55

[8] Akbari-Jeyhouni R., Ochbelagh D.R., Maiorino J.R., D'Auria F., Stefani G. L., The utilization of thorium in Small Modular Reactors – Part I: Neutronic assessment, *Annals of Nuclear Energy* Vol. 120, 2018, pp. 422-30

[9] Gholamzadeh Z., Feghhi S.A., Soltani L., Rezazadeh M., Tenreiro C., Mahdi J., Burn-up calculation of different thorium-based fuel matrixes in a thermal research reactor using MCNPX 2.6 code, *Nukleonika*, vol. 59, 2014, pp. 129-36

[10] International Atomic Energy Agency., Thorium fuel cycle-potential benefits and challenges. Vienna: IAEA-TECDOC-1450, 2005

[11] Organization for Economic Co-operation and Development ECD/NEA., Status Report On Spent Fuel Pools Under Loss-Of-Cooling And Loss-Of-Coolant Accident Conditions. 2015. *Available from: https://www.oecd-nea.org/nsd/docs/2015/csni-r2015-2.pdf*

[12] Eletronuclear - Eletrobrás Termonuclear S.A., Final Safety Analysis Report – *FSAR Angra 2*. Rio de Janeiro, Rev. 13, April, 2013

[13] Achilles J.P., Cardoso F., Faria V., Pereira C., Veloso M., Criticality safety analysis of spent fuel pool for a PWR using UO_2, MOX, (Th-U)O_2 and (TRU-Th)O_2 fuels, *Brazilian Journal of Radiation Sciences,* Vol. 07-03A, 2019, pp. 1-16

[14] Roache P. J., Perspective: A Method for Uniform Reporting of Grid Refinement Studies. *Journal of Fluids Engineering*, Vol. 116, 1994, pp. 405-13

[15] Roache P. J., Fundamentals of verification and validation. Socorro, New Mexico: *Hermosa publishers*, 2009

[16] Dinçer İ and Zamfirescu C., Drying Phenomena: Theory and Applications, 1st ed. United Kingdom: *John Wiley & Sons, Ltd*, 2015, p. 457

[17] International Atomic Energy Agency., Thermophysical properties of materials for nuclear engineering: a tutorial and collection of data. Vienna: *IAEA-THPH*, 2008, p. 28

[18] Oak Ridge National Laboratory. Thermophysical properties of MOX and U02 fuels including the effects of irradiation. Springfield: *ORNL/TM-2000/351*, 2000, p. 11,19,29

[19] International Atomic Energy Agency. Thermophysical properties database of materials for light water reactors and heavy water reactors. Vienna: *IAEA-TECDOC-1496*, 2006, p.185

[20] Kutty T.R.G., Banerjee J., Kumar A., Thermophysical properties of Thoria-based Fuels. Green Energy and Technology; Springer-Verlag London, 2013, p. 34.